

Effects of Large Halides on the Structures of Lanthanide(III) and Plutonium(III) Borates

Matthew J. Polinski,[†] Shuao Wang,[†] Justin N. Cross,[†] Evgeny V. Alekseev,^{‡,§} Wulf Depmeier,^{||} and Thomas E. Albrecht-Schmitt^{*,†}

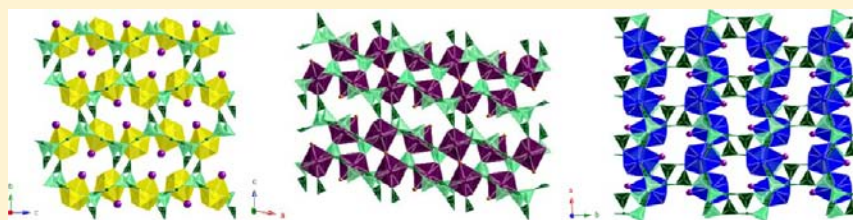
[†]Department of Chemistry and Biochemistry and Department of Civil Engineering and Geological Sciences, University of Notre Dame, 156 Fitzpatrick Hall, University of Notre Dame, Notre Dame, Indiana 46556, United States

[‡]Forschungszentrum Jülich GmbH, Institute for Energy and Climate Research (IEK-6), 52428 Jülich, Germany

[§]Institut für Kristallographie, RWTH Aachen University, D-52066 Aachen, Germany

^{||}Institut für Geowissenschaften, Universität zu Kiel, 24118 Kiel, Germany

S Supporting Information



ABSTRACT: Reactions of LnBr_3 or LnOI with molten boric acid result in formation of $\text{Ln}[\text{B}_5\text{O}_8(\text{OH})(\text{H}_2\text{O})_2\text{Br}]$ ($\text{Ln} = \text{La} - \text{Pr}$), $\text{Nd}_4[\text{B}_{18}\text{O}_{25}(\text{OH})_{13}\text{Br}_3]$, or $\text{Ln}[\text{B}_5\text{O}_8(\text{OH})(\text{H}_2\text{O})_2\text{I}]$ ($\text{Ln} = \text{La} - \text{Nd}$). Reaction of PuOI with molten boric acid yields $\text{Pu}[\text{B}_7\text{O}_{11}(\text{OH})(\text{H}_2\text{O})_2\text{I}]$. The Ln(III) and Pu(III) centers in these compounds are found as nine-coordinate hula-hoop or 10-coordinate capped triangular cupola geometries where there are six approximately coplanar oxygen donors provided by triangular holes in the polyborate sheets. The borate sheets are connected into three-dimensional networks by additional BO_3 triangles and/or BO_4 tetrahedra that are roughly perpendicular to the layers. The room-temperature absorption spectrum of single crystals of $\text{Pu}[\text{B}_7\text{O}_{11}(\text{OH})(\text{H}_2\text{O})_2\text{I}]$ shows characteristic f–f transitions for Pu(III) that are essentially indistinguishable from Pu(III) in other compounds with alternative ligands and different coordination environments.

INTRODUCTION

The lanthanides represent a unique series where fine control of the ionic radius is easily attained while maintaining a single +3 oxidation state. Furthermore, the lanthanide contraction is relatively constant as the series is traversed. The nine-coordinate radii from lanthanum (1.216 Å) to lutetium (1.032 Å) have an approximate 0.02 Å difference for each adjacent element.¹ While examples are known, lanthanide complexes with coordination number 10 are atypical when compared with coordination numbers of eight or nine.^{2,3} Additionally, the most typical geometries for 10-coordinate complexes are the bicapped square antiprism and sphenocorona, while less common geometries are known.² These geometries depend on both the number of different ligands in the system and the differing denticities of those ligands. Those of less common arrangement tend to require a fewer number of ligands with differing denticities.

Borates are among the most structurally diverse polymeric networks and contain BO_3 triangles and/or BO_4 tetrahedra that can corner share to form clusters, chains, sheets, or frameworks.^{4–6} The complexity of these networks can change as a function of numerous experimental conditions such as pH, temperature, stoichiometry, and complexation to the metal

ions. We recently reported on the structures of the trivalent lanthanide and actinide (i.e., Pu(III), Am(III), and Cm(III)) borates when chloride is also present in the reaction.^{7–9} It has been demonstrated that both the lanthanides and the actinides in these borate systems form unusual 9- and 10-coordinate geometries, and these two series do not fully parallel each other even when synthesized under identical reaction conditions.^{7–9}

The chemical differences between the lanthanide and actinide series may be exploitable in terms of storage and separation of nuclear waste. Currently, some of the United States' nuclear defense waste is being stored in a deep geological repository in Carlsbad, NM, known as the Waste Isolation Pilot Plant (WIPP).¹⁰ Once closed, the WIPP repository will become saturated with hydrogen and methane, making it highly reducing, favoring the trivalent state for the lanthanides and tri- and tetravalent states for the later actinides (Pu–Cm).¹¹ The most prevalent anions present in the intergranular salt brines in WIPP are chloride and bromide with the former being present in a larger concentration.¹⁰ Furthermore, it has been demonstrated that borate is the

Received: May 7, 2012

Published: June 26, 2012

primary complexant for trivalent metal ions in the brines at WIPP.¹² Thus, interest in the trivalent lanthanide and actinide borates results from their potential formation in WIPP. We already reported on the structures obtained for the lanthanide and actinide borates when chloride is also in the system,^{7–9} and thus, this follow up article reports on the lanthanide and plutonium species obtained when bromide and iodide are also present. While iodine is not present in significant quantities in the salt brines of WIPP, it has been included for near completeness of the halide series.

EXPERIMENTAL SECTION

Synthesis. $\text{Ln}[\text{B}_5\text{O}_8(\text{OH})(\text{H}_2\text{O})_2\text{Br}]/\text{Nd}_4[\text{B}_{18}\text{O}_{25}(\text{OH})_{13}\text{Br}_3]/\text{Ln}[\text{B}_5\text{O}_8(\text{OH})(\text{H}_2\text{O})_2\text{Br}]$. All reported lanthanide species were synthesized starting with Ln_2O_3 and the appropriate acid (HBr or HI). All starting materials were of reagent grade and used as received without any further purification. Ln_2O_3 (200 mg) was charged into a PTFE-lined Parr 4749 autoclave with a 23 mL internal volume and dissolved with the minimum amount of the appropriate acid and reduced to a moist residue. A 215 μL amount of deionized water was added to the residue along with boric acid (molar ratio 15:1 in favor of boric acid). The sample was sealed and heated at 240 °C for 5 days followed by slow cooling over a 2–3 day period. The resulting products were washed extensively with boiling deionized water to remove the excess boric acid.

$\text{Pu}[\text{B}_7\text{O}_{11}(\text{OH})(\text{H}_2\text{O})_2\text{I}]$. In order to prevent oxidation, synthesis of $\text{Pu}[\text{B}_7\text{O}_{11}(\text{OH})(\text{H}_2\text{O})_2\text{I}]$ was carried out in an Ar-filled glovebox. ²⁴²PuO₂ (10 mg) was charged into a PTFE-lined Parr 4749 autoclave with a 10 mL internal volume, treated with concentrated HI, and reduced to a residue of PuOI. Boric acid (63 mg) was then added along with 30 μL of deionized water. The sample was heated for 5 days at 240 °C followed by cooling to room temperature over a 2 day period. The resulting product consisted of very pale blue (nearly colorless) rectangular tablets.

Caution! ²⁴²Pu ($t_{1/2} = 3.75 \times 10^5$ year) represents a serious health risk owing to its α and γ emission. All studies with plutonium were conducted in a laboratory dedicated to studies on transuranium elements. This laboratory is located in a nuclear science facility and is equipped with HEPA filtered hoods and negative pressure gloveboxes that are ported directly into the hoods. A series of counters continually monitor radiation levels in the laboratory. The laboratory is licensed by the Nuclear Regulatory Commission. All experiments were carried out with approved safety operating procedures. All free-flowing solids are worked with in gloveboxes, and products are only examined when coated with either water or Krytox oil and water. There are significant limitations in accurately determining yield with plutonium compounds because this requires drying, isolating, and weighing a solid, which poses certain risks, as well as manipulation difficulties given the small quantities employed in the reactions.

Crystallographic Studies. Crystals of all compounds were mounted on CryoLoops with Krytox oil and optically aligned on a Bruker APEXII Quazar X-ray diffractometer using a digital camera. Initial intensity measurements were performed using a $1\mu\text{S}$ X-ray source, a 30 W microfocused sealed tube (Mo $K\alpha$, $\lambda = 0.71073$ Å) with high-brilliance and high-performance focusing Quazar multilayer optics. Standard APEXII software was used for determination of the unit cells and data collection control. The intensities of reflections of a sphere were collected by a combination of four sets of exposures (frames). Each set had a different φ angle for the crystal, and each exposure covered a range of 0.5° in ω . A total of 1464 frames were collected with an exposure time per frame of 10–40 s, depending on the crystal. SAINT software was used for data integration including Lorentz and polarization corrections. Semiempirical absorption corrections were applied using the program SCALE (SADABS).¹³ Selected crystallographic information is listed in Tables 1 and 2. Atomic coordinates and additional structural information are provided in the Supporting Information.

Table 1. Crystallographic Data for $\text{La}[\text{B}_5\text{O}_8(\text{OH})(\text{H}_2\text{O})_2\text{Br}]$ (LaBOBr), $\text{Ce}[\text{B}_5\text{O}_8(\text{OH})(\text{H}_2\text{O})_2\text{Br}]$ (CeBOBr), $\text{Pr}[\text{B}_5\text{O}_8(\text{OH})(\text{H}_2\text{O})_2\text{Br}]$ (PrBOBr), and $\text{Nd}_4[\text{B}_{18}\text{O}_{25}(\text{OH})_{13}\text{Br}_3]$ (NdBOBr)

compound	LaBOBr	CeBOBr	PrBOBr	NdBOBr
mass	448.87	450.08	450.87	1619.27
color and habit	colorless, tablet	colorless, tablet	green, tablet	purple, acicular
space group	$P2_1/n$	$P2_1/n$	$P2_1/n$	$P2_1/c$
<i>a</i> (Å)	6.5197(11)	6.4953(14)	6.4910(7)	10.544(5)
<i>b</i> (Å)	15.213(3)	15.159(3)	15.1426(15)	6.451(3)
<i>c</i> (Å)	10.704(2)	10.670(2)	10.6639(11)	23.485(11)
α (deg)	90	90	90	90
β (deg)	90.017(2)	90.048(2)	90.044(1)	97.754(5)
γ (deg)	90	90	90	90
<i>V</i> (Å ³)	1061.6(3)	1050.6(4)	1048.16(19)	1582.9(13)
<i>Z</i>	4	4	4	2
<i>T</i> (K)	100(2)	100(2)	100(2)	127(2)
λ (Å)	0.71073	0.71073	0.71073	0.71073
max 2θ (deg)	26.11	27.52	27.62	27.71
ρ^{calcd} (g cm ⁻³)	2.808	2.846	2.857	3.397
μ (Mo $K\alpha$)	78.34	81.82	85.07	103.80
$R(F)$ for $F_o \geq 2\sigma(F_o)$ ^a	0.0318	0.0297	0.0291	0.0288
$R_w(F_o)$ ^b	0.0585	0.0560	0.0679	0.0566

$${}^a R(F) = \sum \|F_o\| - \|F_c\| / \sum \|F_o\|, \quad {}^b R(F_o) = [\sum w(F_o^2 - F_c^2) / \sum w(F_o^2)]^{1/2}.$$

UV–Vis–NIR Spectroscopy. UV–vis–NIR data were acquired for individual crystals using a Craic Technologies microspectrophotometer. Crystals were placed on quartz slides under Krytox oil, and data were collected from 400 to 1400 nm (Figure 5). The exposure time was auto-optimized by the Craic software.

RESULTS AND DISCUSSION

Structure and Topological Description. $\text{Ln}[\text{B}_5\text{O}_6(\text{OH})_5\text{Br}]$ and $\text{Ln}[\text{B}_5\text{O}_6(\text{OH})_5\text{I}]$. Reaction of early lanthanide halides with boric acid is a facile method in producing lanthanide borates with halogenated metal centers. Depending on the identity of the halide, two isotopic products, $\text{Ln}[\text{B}_5\text{O}_6(\text{OH})_5\text{Br}]$ (Ln = La–Pr) and $\text{Ln}[\text{B}_5\text{O}_6(\text{OH})_5\text{I}]$ (Ln = La–Nd), can be obtained which crystallize in the monoclinic space group, $P2_1/n$.

These compounds form dense, three-dimensional structures (Figure 1b) that extend in the *bc* plane and contain only corner-sharing BO_3 and BO_4 units that create triangular holes (comprised of one BO_4 tetrahedra and two BO_3 triangles) where the lanthanide cations reside. Within the *ac* plane of the three-dimensional framework, layers of lanthanide metal centers can be found that create the sheet topology (Figure 1a). These sheets are tethered to one another by a corner-sharing BO_3 triangle connected to two BO_4 tetrahedra which are in turn coordinated to the lanthanide metal centers in the equatorial plane.

The polyborate sheet topology provides six oxygen donors that are nearly coplanar, which allows for a 10-coordinate geometry that is not typically found for the trivalent lanthanides or actinides. This 10-coordinate geometry (Figure 2a and 2b) is best described as a capped triangular cupola² where the capping group is a bromide or iodide anion and the triangular base is composed of oxygen atoms from the layer tethering BO_3 triangle and two different water molecules. The capping halides are terminal but point toward one another, with an approximate

Table 2. Crystallographic Data for La[B₅O₈(OH)(H₂O)₂I] (LaBOI), Ce[B₅O₈(OH)(H₂O)₂I] (CeBOI), Pr[B₅O₈(OH)(H₂O)₂I] (PrBOI), Nd[B₅O₈(OH)(H₂O)₂I] (NdBOI), and Pu[B₇O₁₁(OH)(H₂O)₂I] (PuBOI)

compound	LaBOI	CeBOI	PrBOI	NdBOI	PuBOI
mass	495.86	497.07	497.86	501.19	668.57
color and habit	colorless, tablet	colorless, tablet	green, tablet	purple, tablet	very pale blue; rectangular
space group	<i>P</i> 2 ₁ / <i>n</i>				
<i>a</i> (Å)	6.5287(10)	6.4983(10)	6.4877(10)	6.4763(5)	8.1103(10)
<i>b</i> (Å)	15.494(2)	15.416(2)	15.392(2)	15.3499(11)	17.060(2)
<i>c</i> (Å)	10.7442(17)	10.7041(16)	10.6857(16)	10.6734(8)	9.7923(13)
α (deg)	90	90	90	90	90
β (deg)	90.353(2)	90.306(2)	90.254(2)	90.3160(10)	90.1330(10)
γ (deg)	90	90	90	90	90
<i>V</i> (Å ³)	1086.8(3)	1072.3(3)	1067.0(3)	1061.03(14)	1354.9(3)
<i>Z</i>	4	4	4	4	4
<i>T</i> (K)	100(2)	100(2)	100(2)	100(2)	100(2)
λ (Å)	0.71073	0.71073	0.71073	0.71073	0.71073
max 2 θ (deg)	27.59	27.50	27.47	28.53	27.48
ρ_{calcd} (g cm ⁻³)	3.030	3.079	3.099	3.137	3.278
μ (Mo <i>K</i> α)	68.16	71.70	75.05	78.49	72.13
<i>R</i> (<i>F</i>) for $F_o^2 > 2\sigma(F_o^2)^a$	0.0316	0.0235	0.0241	0.0214	0.0807
<i>R</i> _w (F_o^2) ^b	0.0615	0.0555	0.0571	0.0485	0.2210

$$^a R(F) = \sum ||F_o| - |F_c|| / \sum |F_o|. \quad ^b R(F_o^2) = [\sum w(F_o^2 - F_c^2)^2 / \sum w(F_o^4)]^{1/2}.$$

separation of 5 Å, which creates a rather large void space in the three-dimensional framework.

For the lanthanide borate bromides, the equatorial bond lengths range from 2.554(4) to 2.653(4) Å, 2.542(3) to 2.641(3) Å, and 2.544(3) to 2.640(3) Å in La[B₅O₈(OH)(H₂O)₂Br] (**LaBOBr**), Ce[B₅O₈(OH)(H₂O)₂Br] (**CeBOBr**), and Pr[B₅O₈(OH)(H₂O)₂Br] (**PrBOBr**), respectively (Table 3). The base bond lengths range from 2.569(4) to 2.615(4) Å, 2.535(4) to 2.596(4) Å, and 2.525(4) to 2.583(4) Å for **LaBOBr**, **CeBOBr**, and **PrBOBr**, respectively, with O9 being the oxygen of the BO₃ unit (Figure 2a). The capping bromide has a bond distance of 3.1253(9), 3.0994(8), and 3.0975(6) Å for **LaBOBr**, **CeBOBr**, and **PrBOBr**, respectively.

For the lanthanide borate iodides, the equatorial bond lengths range from 2.560(4) to 2.698(4) Å, 2.538(3) to 2.685(3) Å, 2.535(3) to 2.677(3) Å, and 2.525(3) to 2.668(3) Å in La[B₅O₈(OH)(H₂O)₂I] (**LaBOI**), Ce[B₅O₈(OH)(H₂O)₂I] (**CeBOI**), Pr[B₅O₈(OH)(H₂O)₂I] (**PrBOI**), and Nd[B₅O₈(OH)(H₂O)₂I] (**NdBOI**), respectively (Table 4). The base bond lengths range from 2.500(4) to 2.595(4) Å, 2.469(3) to 2.568(3) Å, 2.448(3) to 2.552(3) Å, and 2.437(3) to 2.530(3) Å for **LaBOI**, **CeBOI**, **PrBOI**, and **NdBOI**, respectively, with O3 being the oxygen of the BO₃ unit (Figure 2b). The capping iodide has a bond distance of 3.3518(7), 3.3189(6), 3.3037(6), and 3.2847(4) Å for **LaBOI**, **CeBOI**, **PrBOI**, and **NdBOI**, respectively. The decrease in bond lengths from **LaBOBr** to **PrBOBr** and **LaBOI** to **NdBOI** is to be expected as the lanthanide contraction is observed in this system. An approximate 20 Å³ difference in volume is observed in going from the bromide to iodide borate system as would be expected with a much larger capping anion in the latter.

Nd₄[B₁₈O₂₅(OH)₁₃Br₃]. Neodymium represents a transition point in the lanthanide borate bromide series. The product obtained is Nd₄[B₁₈O₂₅(OH)₁₃Br₃] (**NdBOBr**), which crystallizes in the monoclinic space group, *P*2₁/*c*.

This compound also possesses a dense, but different, three-dimensional structure (Figure 3b) as well as a different sheet topology (Figure 3a). Like the aforementioned lanthanide bromide and iodide compounds, corner-sharing BO₃ and BO₄

units create triangular holes; however, in this structure the triangular holes are comprised of two BO₄ tetrahedra and one BO₃ triangle which provide a hole for the metal center. Also, the three-dimensional framework can be viewed in the *ac* plane, while the sheet extends along the *ab* plane.

The neodymium centers possess a bromide anion that is either bridged (Nd2) or terminal (Nd1) (Figure 2c). All centers are nine coordinate with a geometry best described as a hula hoop (Figure 2c).³ The polyborate network provides six oxygen atoms that are nearly coplanar, and the additional ligands are two additional oxygens from either two BO₄ groups (bridged center) or an oxygen from a BO₃ group and a hydroxide (nonbridged center). The layers are connected to one another by a corner-sharing BO₃ triangle connected to two BO₄ tetrahedra which are coordinated to the neodymium metal centers in the equatorial plane as seen in the **LaBOBr**, **CeBOBr**, and **PrBOBr** structures. Unlike the other bromide cohorts, **NdBOBr** also has the additional tethering of layers by use of the bridging bromide (Figures 2c and 3b).

The Nd–Br bond length in the bridged **NdBOBr** center is 2.9144(13) Å, while the terminal anion center has a Nd–Br bond length of 2.9618(12) Å. The equatorial bond lengths range from 2.504(4) to 2.685(4) Å and base lengths from 2.400(4) to 2.482(4) Å in the bridged **NdBOBr** metal centers, while the unbridged metal centers have equatorial bond lengths of 2.498(4)–2.601(4) Å and base lengths of 2.482(4)–2.493(4) Å (Table 5).

Pu[B₇O₁₁(OH)(H₂O)₂I]. The plutonium(III) borate iodide, Pu[B₇O₁₁(OH)(H₂O)₂I] (**PuBOI**), is unique when compared to not only the lanthanide borate iodides but also the other halogen-containing plutonium(III) borates. **PuBOI** was refined in the monoclinic space group *P*2₁/*n*. Like the metal centers in the lanthanide borate iodides above, the plutonium center is 10 coordinate with the capped triangular cupola geometry (Figure 2b). The polyborate sheet topology provides six oxygen donors that are nearly coplanar, an apical and a terminal iodine, and base sites comprised of oxygens from two different water (O1 and O2) moieties as well as a BO₃ triangle (O3). The coordination to the plutonium is shown in Figure 2b. The sheet

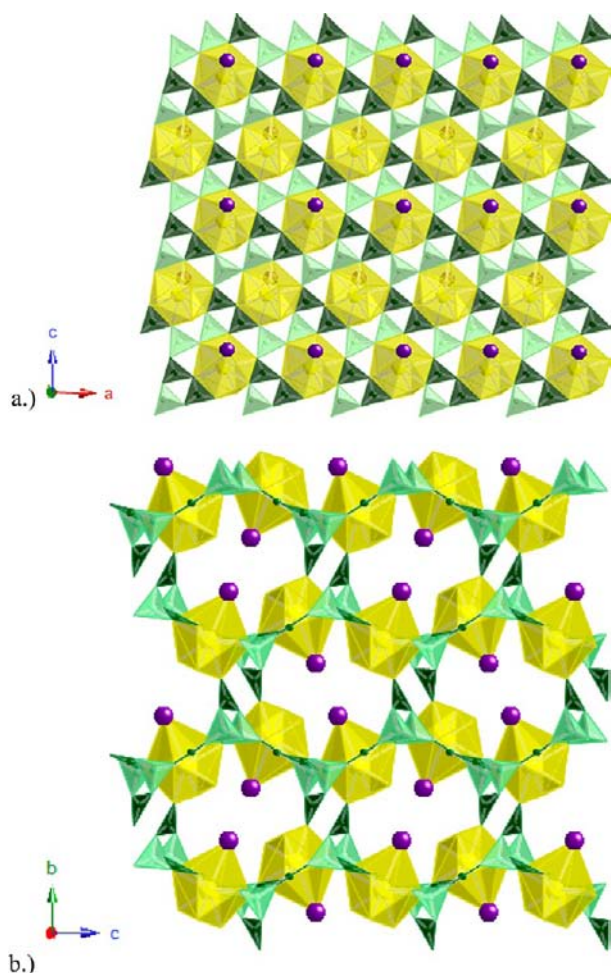


Figure 1. Depiction of the (a) sheet topology and (b) three-dimensional framework of $\text{La}[\text{B}_5\text{O}_8(\text{OH})(\text{H}_2\text{O})_2\text{Br}]$ ($\text{Ln} = \text{La}-\text{Pr}$) and $\text{La}[\text{B}_5\text{O}_8(\text{OH})(\text{H}_2\text{O})_2\text{I}]$ ($\text{Ln} = \text{La}-\text{Nd}$). Lanthanide metal centers are depicted by the yellow polyhedra, the halide (Br and I) is depicted by the purple spheres, BO_4 tetrahedra are depicted as light green units, and BO_3 triangles are depicted as dark green units.

topology, which extends in the ac plane, is comprised of two BO_3 triangles and a BO_4 tetrahedron that creates a triangular hole for the plutonium center to reside (Figure 4a). The most noticeable feature of the sheet topology is the presence of a μ_3 oxygen atom that is corner shared between three BO_4 units.

Bound to the base of the plutonium metal center is a BO_3 triangle that is corner shared to a BO_3 triangle bound to the μ_3 BO_4 unit which is connected in the equatorial plane of another plutonium center. This connectivity allows for the sheets to be tethered together, creating the three-dimensional framework which extends in the ab plane (Figure 4b). Iodine atoms are staggered in such a manner that creates rather large void spaces in the three-dimensional structure, which is also observed in the LnBOBr and LnBOI structures above. Furthermore, an additional BO_3 triangle is needed to not only create sufficient space for the iodide anions but also tether the layers together.

The equatorial bond lengths in **PuBOI** range from 2.523(18) to 2.696(17) Å, while the base bond lengths range from 2.50(2) to 2.70(2) Å (Table 6). The longest bond length on the base sites (O3) is the BO_3 unit, which is used to tether the layers together. The Pu–I bond length is 3.350(2) Å and is similar to what is observed in the LnBOI structures presented above.

The room-temperature absorption spectrum for $\text{Pu}[\text{B}_7\text{O}_{11}(\text{OH})(\text{H}_2\text{O})_2\text{I}]$ can be seen in Figure 5. The spectrum displays a vast series of Laporte forbidden f–f transitions throughout the UV–vis–NIR region. These f–f transitions have been carefully assigned by Carnall and co-workers,¹⁴ and we used this analysis to assign the transitions shown. The most important transition that occurs for Pu(III) is the ${}^6\text{H}_{5/2} \rightarrow {}^6\text{H}_{13/2}$ transition near 900 nm. Fortunately this region is bare for Pu(IV). The ${}^6\text{H}_{5/2} \rightarrow {}^4\text{L}_{13/2}$ and ${}^6\text{H}_{5/2} \rightarrow {}^4\text{M}_{15/2}$ transitions are also routinely used to identify Pu(III). The absorption spectrum obtained is virtually indistinguishable from other Pu(III) compounds with different ligands and coordination environments.^{7,15,16}

While the crystals of $\text{Pu}[\text{B}_7\text{O}_{11}(\text{OH})(\text{H}_2\text{O})_2\text{I}]$ are large and well formed with clearly defined edges, faces, and corners, and the crystals diffract remarkably well without any indication of twinning, refinement of the structure yields somewhat high residuals and nonpositive definite thermal parameters even with moderate restraints owing primarily to disorder of iodide in the structure. After approximately 1 week postsynthesis, the crystals of $\text{Pu}[\text{B}_7\text{O}_{11}(\text{OH})(\text{H}_2\text{O})_2\text{I}]$, while giving no visual indication of loss of crystallinity, did not diffract. It is apparent that radiolysis rapidly destroys the Pu–I bond and is observed immediately upon isolation of crystals. This radiolysis leads to disorder in the crystal. This type of radiation damage has not been observed in any other Pu(III) borate to date. Furthermore, the UV–vis–NIR spectrum shows no indication of the presence of Pu(IV); and thus, this compound is air stable and oxidation is not an issue. Owing to some disorder, the structure reported in this work does not have the highly precise metrics that we are accustomed to. However, given the scarcity of plutonium structures and the fact that this is the only Pu(III) borate iodide, we think that its inclusion in the work is justified.

Periodic Trends. The lanthanide borate series obtained from having either bromide or iodide present in the system parallel each other nicely, while comparisons to the plutonium borates with either bromide or iodide are not as straightforward. We recently reported on the structure of the first plutonium(III) borate, $\text{Pu}_2[\text{B}_{12}\text{O}_{18}(\text{OH})_4\text{Br}_2(\text{H}_2\text{O})_3] \cdot 0.5\text{H}_2\text{O}$, which contains two crystallographically unique plutonium centers.¹⁵ Each metal center contains a capping, terminal bromide anion; however, both the capped triangular cupola and the hula-hoop geometries are observed. This is a result of the borate network providing six near coplanar oxygen donors in the equatorial plane of the plutonium which allows for these unusual geometries. The base sites on both the 9- and the 10-coordinate centers are comprised of oxygens from waters attached to the metal centers. This is different than what is observed for either $\text{Ln}[\text{B}_5\text{O}_6(\text{OH})_5\text{Br}]$ ($\text{Ln} = \text{La}-\text{Pr}$) or $\text{Nd}_4[\text{B}_{18}\text{O}_{25}(\text{OH})_{13}\text{Br}_3]$ as the former has base sites comprised of oxygens from water molecules and a BO_3 unit and the later is comprised of either all BO_4 units (bridged center) or BO_3 units and a hydroxide (nonbridged center).

It is interesting to note that the bromide anion is only bridging in the **NdBOBr** structure, and this bridging mode is not observed in the $\text{Pu}_2[\text{B}_{12}\text{O}_{18}(\text{OH})_4\text{Br}_2(\text{H}_2\text{O})_3] \cdot 0.5\text{H}_2\text{O}$ structure.¹⁵ The bridging nature of the halide is also observed in $\text{Sm}_4[\text{B}_{18}\text{O}_{25}(\text{OH})_{13}\text{Cl}_3]$ and $\text{Eu}_4[\text{B}_{18}\text{O}_{25}(\text{OH})_{13}\text{Cl}_3]$, which are isotopic to **NdBOBr** and similar to what is seen in $\text{Ln}[\text{B}_4\text{O}_6(\text{OH})_2\text{Cl}]$ ($\text{Ln} = \text{La}-\text{Nd}$)^{7,17} and $\text{Pu}[\text{B}_4\text{O}_6(\text{OH})_2\text{Cl}]$ ⁷ though **NdBOBr** contains only one bridging, apical bromide. Also, $\text{Pu}_2[\text{B}_{12}\text{O}_{18}(\text{OH})_4\text{Br}_2(\text{H}_2\text{O})_3] \cdot 0.5\text{H}_2\text{O}$ has plutonium centers with two different geometries, while the LnBOBr

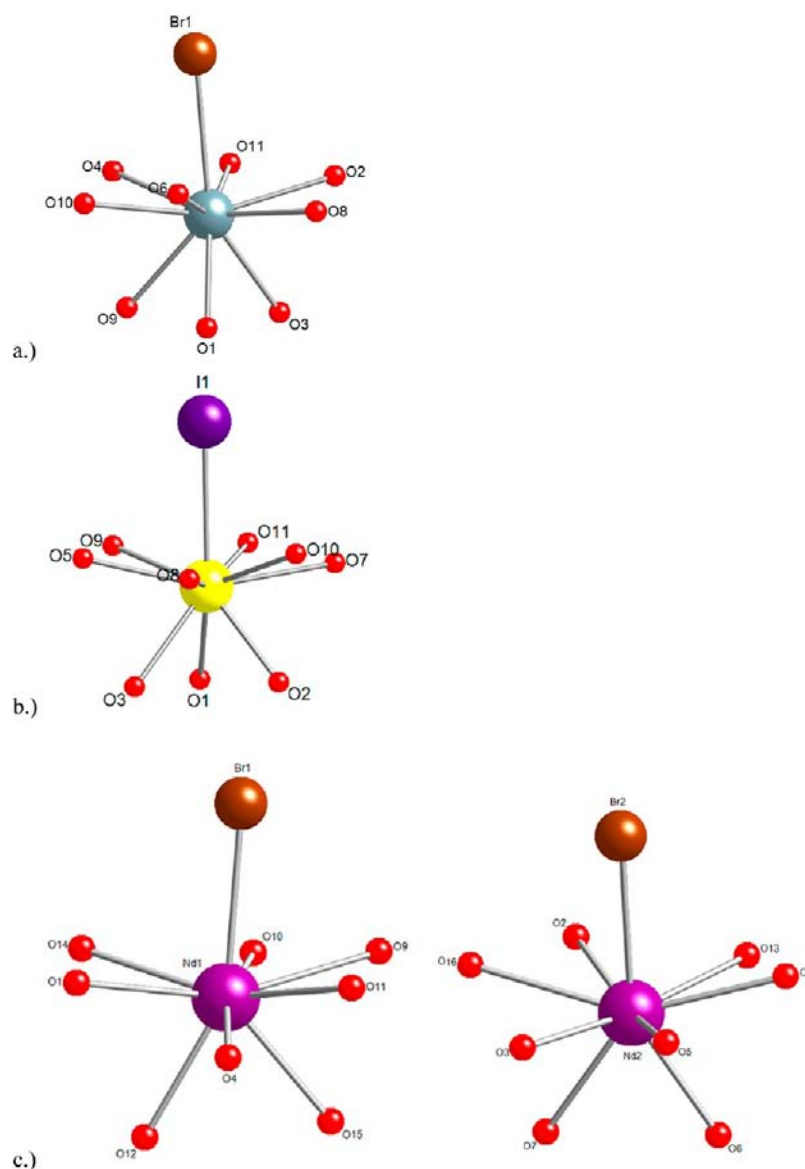


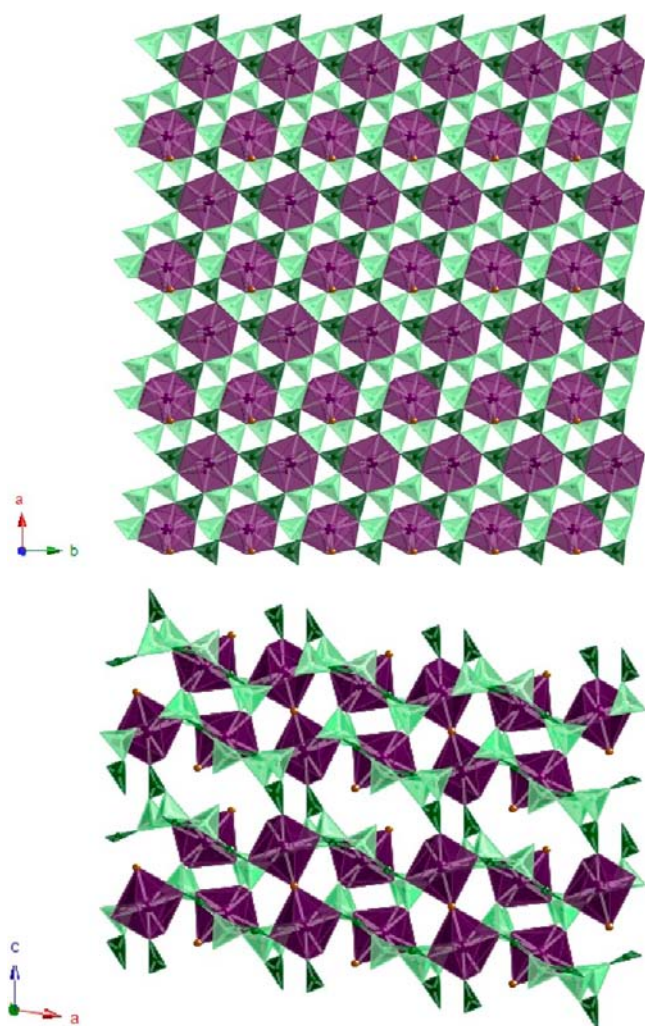
Figure 2. Coordination geometries for the lanthanide and actinide metal centers. (a) Capped triangular cupola depicting coordination of $\text{La}[\text{B}_5\text{O}_8(\text{OH})(\text{H}_2\text{O})_2\text{Br}]$ ($\text{Ln} = \text{La}-\text{Pr}$), (b) capped triangular cupola depicting coordination of $\text{La}[\text{B}_5\text{O}_8(\text{OH})(\text{H}_2\text{O})_2\text{I}]$ ($\text{Ln} = \text{La}-\text{Nd}$) and $\text{Pu}[\text{B}_7\text{O}_{11}(\text{OH})(\text{H}_2\text{O})_2\text{I}]$, and (c) hula hoop depicting coordination of $\text{Nd}_4[\text{B}_{18}\text{O}_{25}(\text{OH})_{13}\text{Br}_3]$.

Table 3. Selected Bond Distances (Angstroms) for $\text{La}[\text{B}_5\text{O}_8(\text{OH})(\text{H}_2\text{O})_2\text{Br}]$ (LaBOBr), $\text{Ce}[\text{B}_5\text{O}_8(\text{OH})(\text{H}_2\text{O})_2\text{Br}]$ (CeBOBr), and $\text{Pr}[\text{B}_5\text{O}_8(\text{OH})(\text{H}_2\text{O})_2\text{Br}]$ (PrBOBr)

equatorial		base		equatorial		base	
La(1)–Br(1)	3.1253(9)	La(1)–O(1)	2.569(4)	Pr(1)–Br(1)	3.0975(6)	Pr(1)–O(1)	2.525(4)
La(1)–O(2)	2.630(4)	La(1)–O(3)	2.615(4)	Pr(1)–O(2)	2.544(3)	Pr(1)–O(3)	2.583(4)
La(1)–O(4)	2.554(4)	La(1)–O(9)	2.571(4)	Pr(1)–O(4)	2.617(4)	Pr(1)–O(9)	2.553(3)
La(1)–O(6)	2.611(4)			Pr(1)–O(6)	2.588(4)		
La(1)–O(8)	2.653(4)			Pr(1)–O(8)	2.640(3)		
La(1)–O(10)	2.631(4)			Pr(1)–O(10)	2.613(3)		
La(1)–O(11)	2.603(4)			Pr(1)–O(11)	2.572(4)		
Ce(1)–Br(1)	3.0994(8)	Ce(1)–O(1)	2.535(4)				
Ce(1)–O(2)	2.542(3)	Ce(1)–O(3)	2.596(4)				
Ce(1)–O(4)	2.617(3)	Ce(1)–O(9)	2.557(3)				
Ce(1)–O(6)	2.591(3)						
Ce(1)–O(8)	2.641(3)						
Ce(1)–O(10)	2.621(3)						
Ce(1)–O(11)	2.573(3)						

Table 4. Selected Bond Distances (Angstroms) for La[B₅O₈(OH)(H₂O)₂I] (LaBOI), Ce[B₅O₈(OH)(H₂O)₂I] (CeBOI), Pr[B₅O₈(OH)(H₂O)₂I] (PrBOI), and Nd[B₅O₈(OH)(H₂O)₂I] (NdBOI)

equatorial		base		equatorial		base	
La(1)–I(1)	3.3518(7)	La(1)–O(1)	2.582(4)	Pr(1)–I(1)	3.3037(6)	Pr(1)–O(1)	2.544(3)
La(1)–O(5)	2.629(4)	La(1)–O(2)	2.500(4)	Pr(1)–O(5)	2.589(3)	Pr(1)–O(2)	2.448(3)
La(1)–O(7)	2.698(4)	La(1)–O(3)	2.595(4)	Pr(1)–O(7)	2.677(3)	Pr(1)–O(3)	2.552(3)
La(1)–O(8)	2.636(4)			Pr(1)–O(8)	2.610(3)		
La(1)–O(9)	2.611(4)			Pr(1)–O(9)	2.554(3)		
La(1)–O(10)	2.650(4)			Pr(1)–O(10)	2.639(3)		
La(1)–O(11)	2.560(4)			Pr(1)–O(11)	2.535(3)	Nd(1)–O(1)	2.530(3)
Ce(1)–I(1)	3.3189(6)	Ce(1)–O(1)	2.562(3)	Nd(1)–I(1)	3.2847(4)	Nd(1)–O(2)	2.437(3)
Ce(1)–O(5)	2.601(3)	Ce(1)–O(2)	2.469(3)	Nd(1)–O(5)	2.589(3)	Nd(1)–O(3)	2.530(3)
Ce(1)–O(7)	2.685(3)	Ce(1)–O(3)	2.568(3)	Nd(1)–O(7)	2.668(3)		
Ce(1)–O(8)	2.620(3)			Nd(1)–O(8)	2.598(2)		
Ce(1)–O(9)	2.575(3)			Nd(1)–O(9)	2.544(3)		
Ce(1)–O(10)	2.642(3)			Nd(1)–O(10)	2.640(3)		
Ce(1)–O(11)	2.538(3)			Nd(1)–O(11)	2.525(3)		

**Figure 3.** Depiction of the (a) sheet topology and (b) three-dimensional framework of Nd₄[B₁₈O₂₅(OH)₁₃Br₃]. Neodymium metal centers are depicted by the purple spheres, bromine is depicted by the brown spheres, BO₄ tetrahedra are depicted as light green units, and BO₃ triangles are depicted as dark green units.

structures contain solely 10-coordinate centers. Furthermore, the three-dimensional framework, sheet topology, and space group (*Pn*) seen in Pu₂[B₁₂O₁₈(OH)₄Br₂(H₂O)₃].0.5H₂O are

Table 5. Selected Bond Distances (Angstroms) for Nd₄[B₁₈O₂₅(OH)₁₃Br₃] (NdBOBr)

unbridged		bridged	
Nd(1)–Br(1)	2.9618(12)	Nd(2)–Br(2)	2.9144(13)
Nd(1)–O(1)	2.567(4)	Nd(2)–O(2)	2.511(4)
Nd(1)–O(4)	2.498(4)	Nd(2)–O(3)	2.550(4)
Nd(1)–O(9)	2.601(4)	Nd(2)–O(5)	2.504(4)
Nd(1)–O(10)	2.468(4)	Nd(2)–O(6)	2.400(4)
Nd(1)–O(11)	2.523(4)	Nd(2)–O(7)	2.482(4)
Nd(1)–O(12)	2.493(4)	Nd(2)–O(8)	2.543(4)
Nd(1)–O(14)	2.527(4)	Nd(2)–O(13)	2.659(4)
Nd(1)–O(15)	2.482(4)	Nd(2)–O(16)	2.685(4)

different than those of the LnBOBr species presented above. It should be noted that identical experimental conditions were used throughout. A more thorough analysis of the Pu₂[B₁₂O₁₈(OH)₄Br₂(H₂O)₃].0.5H₂O structure can be found elsewhere.¹⁵

PuBOI also has both similarities and differences to the LnBOI species presented. The oxygen base sites of PuBOI and LnBOI (Ln = La–Nd) contain oxygens from a BO₃ group and two different water molecules. While both BO₃ and BO₄ units are necessary to tether the layers together in the LnBOI and PuBOI systems, the arrangement of such is different, leading to a differing three-dimensional framework. Additionally, it takes four BO₃ units to tether the layers in PuBOI, while the LnBOI structures only require two BO₃ units. The mode of tethering the layers in the LnBOBr and LnBOI structures is more similar to what is observed in the Pu₂[B₁₂O₁₈(OH)₄Br₂(H₂O)₃].0.5H₂O structure. The sheet topology of PuBOI is identical to that of Pu₂[B₁₂O₁₈(OH)₄Br₂(H₂O)₃].0.5H₂O and different from that of any of the LnBOBr and LnBOI structures. This sheet topology is also observed in other actinide borates that we prepared^{7–9,18} as well as in the lanthanide borate systems, Ln[B₈O₁₁(OH)₅] (Ln = La–Nd) and Ln[B₉O₁₃(OH)₄] (Ln = Pr–Eu).¹⁹

This work demonstrates the potential halogenated lanthanide/plutonium borates that could form in the geological repository (WIPP) once the lanthanide/plutonium species come into contact with the borate-rich salt brines. It is our hope that these materials prove to be radiation damage resistant and thus may be used as a long-term storage option.

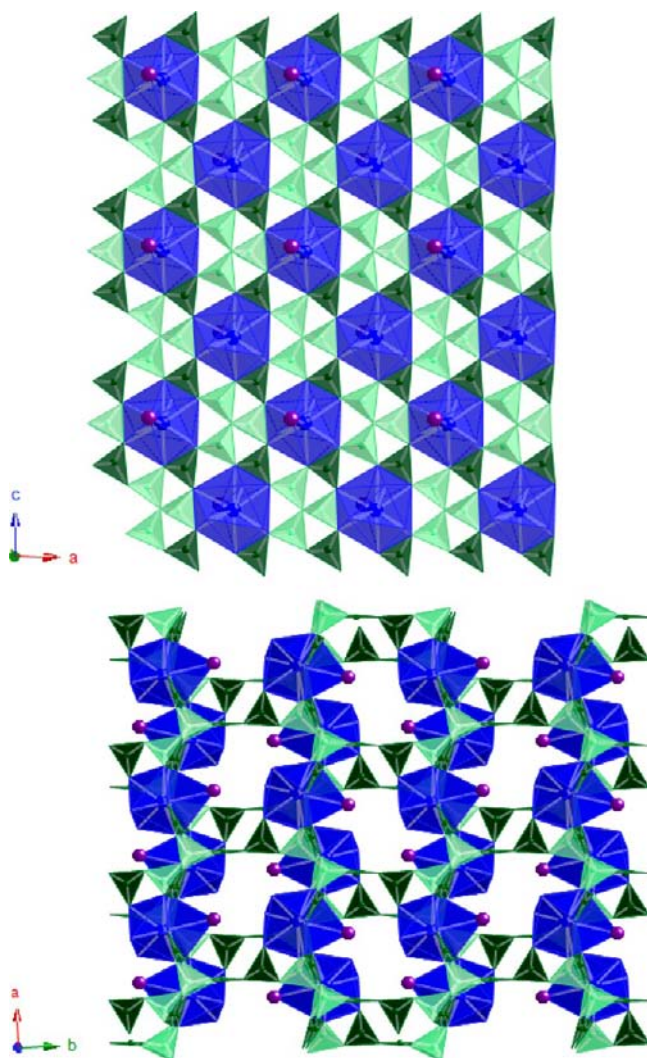


Figure 4. Depiction of the (a) sheet topology and (b) three-dimensional framework of $\text{Pu}[\text{B}_7\text{O}_{11}(\text{OH})(\text{H}_2\text{O})_2\text{I}]$. Plutonium metal centers are depicted by the blue spheres, iodine is depicted by the purple spheres, BO_4 tetrahedra are depicted as light green units, and BO_3 triangles are depicted as dark green units.

Table 6. Selected Bond Distances (Angstroms) for $\text{Pu}[\text{B}_7\text{O}_{11}(\text{OH})(\text{H}_2\text{O})_2\text{I}]$ (PuBOI)

equatorial		base	
Pu(1)–I(1)	3.350(2)	Pu(1)–O(1)	2.55(2)
Pu(1)–O(5)	2.696(17)	Pu(1)–O(2)	2.50(2)
Pu(1)–O(7)	2.523(18)	Pu(1)–O(3)	2.70(2)
Pu(1)–O(8)	2.594(16)		
Pu(1)–O(9)	2.525(17)		
Pu(1)–O(10)	2.563(17)		
Pu(1)–O(11)	2.599(18)		

CONCLUSIONS

In this report we found that, under the same experimental conditions, the lanthanide(III) and plutonium(III) borate systems, in the presence of either bromine or iodine, do not parallel each other and show substantial differences. Thus, use of lanthanides as surrogates for the actinides in the borate system is ill advised as the lanthanide and actinide series are chemically distinct.

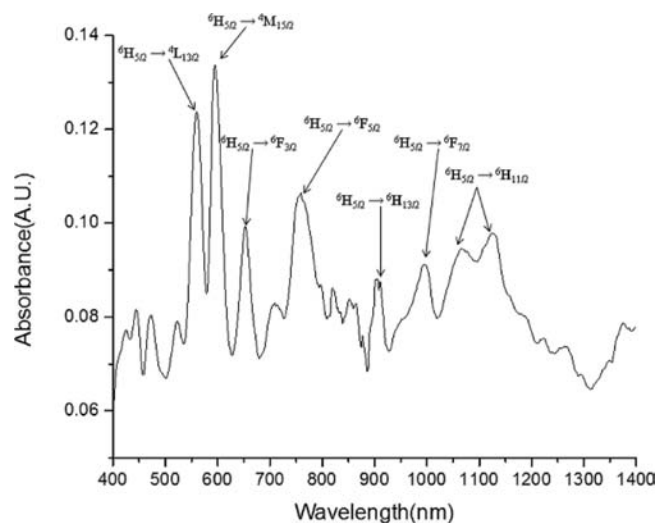


Figure 5. Absorption spectra of $\text{Pu}[\text{B}_7\text{O}_{11}(\text{OH})(\text{H}_2\text{O})_2\text{I}]$ showing $f-f$ transitions that are diagnostic for Pu(III) ($f-f$ transitions are assigned based on ref 14).

Furthermore, the lanthanide borate bromide and iodide series more closely resemble each other than they do to the previously reported lanthanide borate chloride series.^{7–9} It is important to note that in this study reactions with the other lanthanides (Sm–Lu) with both bromine and iodine failed to produce crystalline material. However, our previous report with the lanthanide borate chlorides provided a means of synthesizing $\text{Ln}[\text{B}_6\text{O}_9(\text{OH})_3]$ (Ln = Eu–Lu) when chlorine was present in the system.^{7,20,21}

It is our conclusion that while the borate network helps direct the unusual geometries observed, the counteranions play a role, due to size and/or coordination, in how the layers are tethered to yield the resulting three-dimensional structure. Moreover, the halides have the ability to be either terminal or bridging. The plutonium borate systems are more similar to each other than they are to the lanthanide borates, which represents a difference in their chemical behavior. It appears that further functionalizing the capping groups in these systems may provide a means of new and unusual networks in the borate system.

ASSOCIATED CONTENT

Supporting Information

Crystallization information files (CIF). This material is available free of charge via the Internet at <http://pubs.acs.org>.

AUTHOR INFORMATION

Corresponding Author

*E-mail: talbrec1@nd.edu.

Notes

The authors declare no competing financial interest.

ACKNOWLEDGMENTS

We are grateful for support provided by the Chemical Sciences, Geosciences, and Biosciences Division, Office of Basic Energy Sciences, Office of Science, Heavy Elements Chemistry Program, and U.S. Department of Energy, under Grant DE-FG-09ER16026. The German group was supported via the Helmholtz Association, grant no. VH-NG-815.

■ REFERENCES

- (1) Shannon, R. D. *Acta Crystallogr., Sect. A* **1976**, *32*, 751–767.
- (2) Ruiz-Martínez, A.; Alverz, S. *Chem.—Eur. J.* **2009**, *15*, 7470–7480.
- (3) Ruiz-Martínez, A.; Casanova, D.; Alverz, S. *Chem.—Eur. J.* **2008**, *14*, 1291–1303.
- (4) Burns, P. C.; Grice, J. D.; Hawthorne, F. C. *Can. Mineral* **1995**, *33*, 1131.
- (5) Grice, J. D.; Burns, P. C.; Hawthorne, F. C. *Can. Mineral* **1999**, *37*, 731.
- (6) Yuan, G.; Xue, D. *Acta Crystallogr.* **2007**, *B63*, 353.
- (7) Polinski, M. J.; Grant, D. J.; Wang, S.; Alekseev, E. V.; Cross, J. N.; Villa, E. M.; Depmeier, W.; Gagliardi, L.; Albrecht-Schmitt, T. E. *J. Am. Chem. Soc.* **2012**, Accepted.
- (8) Polinski, M. J.; Wang, S.; Alekseev, E. V.; Depmeier, W.; Albrecht-Schmitt, T. E. *Angew. Chem., Int. Ed.* **2011**, *50*, 8891–8894.
- (9) Polinski, M. J.; Wang, S.; Alekseev, E. V.; Depmeier, W.; Liu, G.; Haire, R. G.; Albrecht-Schmitt, T. E. *Angew. Chem., Int. Ed.* **2012**, *51*, 1869–1872.
- (10) Snider, A. C. *Verification of the Definition of Generic Weep Brine and the Development of a Recipe for this Brine*; ERMS 527505; Sandia National Laboratories: Carlsbad, NM, 2003.
- (11) *Compliance Recertification Application for the Waste Isolation Pilot Plant Appendix SOTERM 2009*; United States Department of Energy, 2009.
- (12) Borkowski, M.; Richmann, M.; Reed, D. T.; Xiong, Y. *Radiochim. Acta* **2010**, *98*, 577–582.
- (13) Sheldrick, G. M. *Acta Crystallogr.* **1995**, *A51*, 33.
- (14) Carnall, W. T.; Fields, P. R.; Pappalardo, R. G. *J. Chem. Phys.* **1970**, *53*, 2922.
- (15) Wang, S.; Alekseev, E. V.; Depmeier, W.; Albrecht-Schmitt, T. E. *Inorg. Chem.* **2011**, *50*, 2079–2081.
- (16) Matonic, J. H.; Scott, B. L.; Neu, M. P. *Inorg. Chem.* **2001**, *40*, 2638–2639.
- (17) Belokoneva, E. L.; Stefanovich, S.; Dimitrova, O. V.; Ivanova, A. *G. Zh. Neorg. Khim.* **2002**, *47*, 370–377.
- (18) Wang, S.; Alekseev, E. V.; Depmeier, W.; Albrecht-Schmitt, T. E. *Chem. Commun.* **2011**, *47*, 10874–10885.
- (19) Li, L.; Jin, X.; Li, G.; Wang, Y.; Liao, F.; Tao, G.; Lin, J. *Chem. Mater.* **2003**, *15*, 2253–2260.
- (20) Lu, P.; Wang, Y.; Lin, J.; You, L. *Chem. Commun.* **2001**, 1178–1179.
- (21) Li, L.; Lu, P.; Wang, Y.; Jin, X.; Li, G.; Wang, Y.; You, L.; Lin, J. *Chem. Mater.* **2002**, *14*, 4963–4968.